BEHAVIOUR OF CONVENTIONAL AND NON-CONVENTIONAL SPEED REGULATING SYSTEMS FOR MARINE DIESEL ENGINES

S. Youssef, M. Hanafi and M. Morsy
Department of Marine Engineering and Naval Architecture, Faculty of Engineering,
Alexandria University, Alexandria, Egypt.

ABSTRACT

The establishment of control engineering technology has urged scientists to develop new techniques whose merits overweigh those of traditional controllers. Two of the recent algorithms in modern control strategy are Pseudo derivative feedback and proportional minus delay control that capture the advantages of conventional controllers and discard their undesired demerits. In this paper, the speed control of the naturally - aspirated marine Diesel engine is investigated when operating with traditional, non - conventional and optimal regulators. Apart from optimal controller, parameter optimization concept according to the integral of the squares of error optimization index is applied. The influence of changing the mean piston speed and the brake mean effective pressure and controllers gains on absolute and relative stability problems, time domain dynamic behaviour and frequency response is considered too.

Keywords: Diesel engines, Traditional controllers, Pseudo derivative feedback control, Proportional minus delay control, State space methods, Parseval's parameter - optimized control, Riccati optimal regulator.

NOMENCLATURE

[A]	System matrix of plant.	
[a]	Closed loop Riccati system matrix = [A] - [B][α]	
[B]	Control vector.	
bmp	Brake mean effective pressure	(Pa).
C_1	$=\dot{m}_o/u_o$	(kg/s/% rack stroke).
C_2	$=\dot{m}_o/\omega_{e,o}$	(kg).
C_3	$= P_{eo}/\dot{m}_o$	(Joule/kg).
C_4	$= \eta_{tr}.\ \eta_p/I\omega_{e,o}$	(s/kg.m^2).
C_5	$= 1/I\omega_{e,o}$	(s/kg.m^2).
C_6	$= 3\eta_{tr}.\eta_p.\ P_{eo}/\omega_{e,o}$	(Joule).
C_f	$= 2\ (2\pi\ C_g/60)^2$	
C_r	= Governor arms ratio, > 1	
Den(s)	Polynomial denominator of $E_1(s)$	
e_1 (t)	or $E_1(s)$ Error signal in time or Laplace domain	
G(s)	Forward path transfer function.	
G_m	Gain margin.	
H(s)	Transfer function of feedback elements.	
h_1	Dead time of proportional minus delay (PMD) governor (s)	
I	Mass polar moment of inertia of rotating parts	(kg.m^2)
[Ī]	Unity matrix.	
J	Quadratic performance index	
J_4	ISE index of third over fourth order polynomials of $E_1(s)$	
j	$=\sqrt{-1}$	
k_1	Gain of open loop transfer function	
k_2	$=\partial z/\partial n_i\|_o$	(cm/rpm)
k_4	$= 2C_f\ C_r\ M\ R_o\ n_o$	(N/rpm).
k_d	Gain of derivative action of speed governor (s).	
k_I	Gain of integral action of speed governor (s^{-1})	
k_m	Gain of proportional minus delay (PMD) governor.	(s)
k_p	Gain of proportional action of speed governor.	
k_s	Spring constant of the centrifugal governor	(N/cm).
[L]	Output row vector.	
M	Mass of one of the centrifugal balls	(kg).
M_p	Percentage maximum overshoot.	
M_r	Resonant peak	(db).
$\dot{m}_f$	Rate of fuel injected into the cylinder	(Kg/s).
$\dot{m}_j$	Rate of fuel delivered by fuel pump	(kg/s).

$\dot{m}_o$	Nominal value of $\dot{m}_f$	(kg/s).
mps	Mean piston speed	(m/s).
Num(s)	Polynomial numerator of E_1	(s).
n	Rate of revolutions of the Diesel engine.	(rpm).
n_i	Desired speed from Diesel engine (command signal)	(rpm).
[O]	Null matrix	
o	Suffix indicating the nominal value.	
P_m	Phase margin	(degrees).
P_e	Brake power	(w).
P_l	Power absorbed by the propeller	(w)
[Q]	Positive definite (or positive-semi definite) real symmetric matrix.	
R	Radius of rotation of fly balls	(cm).
$[r_1]$	Positive - definite real symmetric matrix	
s	Laplace operator	(s^{-1}).
$[...]^T$	Transpose of a matrix.	
t	Time (s).	
[U(t)]	Control vector	
u	Fuel rack position	(%).
[X(t)]	State variable vector.	
y_o	Maximum stroke of fuel rack	(cm).
z_1	Dummy parameter for state matrix derivation.	
$[\alpha]$	= [α_1 α_2 α_3] Proportional state variable feedbacks.	
Δ ...	Change in ...	
$[\xi(t)]$	Desired state vector.	
η_p	Propeller efficiency behind ship.	
$\eta_{p.o.w}$	Propeller efficiency in open water.	
η_{rr}	Relative rotative efficiency.	
η_{tr}	Transmission efficiency of propulsion shaft.	
η_{vol}	Volumetric efficiency of Diesel engine.	
λ	Excess air factor of Diesel engine.	
λ_1	Lagrange multiplier, a positive constant indicating the weight of control cost w.r.t. the minimized errors.	
τ	Delay time constant in controller	(s).
τ_c	Delay time of fuel	(s).
τ_d	Transportation lag of fuel	(s).
ω	Frequency of input/output	(rad/s).
ω_1	Gain cross-over frequency	(rad/s).
ω_e	Angular speed of Diesel engine	(rad/s).
ω_π	Phase cross-over frequency	(rad/s).

INTRODUCTION

In [1], the dynamics of naturally aspirated marine Diesel engine with proportional plus derivative speed regular were analyzed in a parametric study which represents a portion of a research thesis. Among the varied parameters namely: the brake mean effective pressure (bmp), the mean piston speed (mps), the excess air factor (λ) and the volumetric efficiency (η_{vol}) it was concluded that (mps) and (bmp) assumed a considerable and significant influence on the automatic speed control loop with respect to the stability problem, time and frequency domains specifications. In the present research , the dynamic behaviour of various types of traditional and non-conventional controllers namely: P, PD, PI, PDF, PMD and the optimal linear quadratic state feedback regulator obtained from the reduced matrix Riccati equation is investigated w.r.t. the command signal (desired speed) when operating with the marine Diesel engine. Parameter optimization concept is considered in order to minimize the error signal in accordance with the integral of the squares of error [ISE] adopting Parseval's theorem. This is applied to the reference case number 1 [1], and in case of multiple-valued solutions, a comparison is held to decide which of which best suits the reference case. The established solution is then applied to cases number 1,5 and 9 of the plant [1] representing the strong dynamic effect of (mps) and (bmp). It is worthmentioning that conventional controllers (P,I,D,PI,PD and PID) are widely discussed in [2], the non-traditional Pseudo derivative feedback (PDF) is analyzed in [3,4] while the non-conventional proportional minus delay control (PMD) is presented in [5]. The application of Parseval's theorem to quotient of polynomials of the error signal in Laplace domain is treated in [6,7], whereas the principles of optimal linear quadratic regulator design are demonstrated in [8]. In [9,10], an introductory study of conventional, non-conventional, parameter optimized and optimal speed regulators of marine Diesel engines is presented too.

This research is carried out by aid of the powerful symbolic, artificial intelligence-oriented package [11] and the package [12] oriented to numerical computational assistance for analysis and synthesis of control systems.

NUMERICAL TREATMENT :

1- *Regulation with $(PD)_1$ or P_1 controller*

In [1], a specific $(PD)_1$ controller ($k_p = 4$, $k_d = 1$ s) has been chosen for the investigation of the dynamic response of the naturally-aspirated marine Diesel engine when (mps), (bmp), λ and η_{vol} are changed. Since the major influence has been displayed to be of (mps) and (bmp), only the parametric variation in the latter two variables is going to be studied for $k_p = 4$ and 10, while $k_d = 0$, 0.5, 1 and 2 s, with $y_o = 6$ cm, $\tau = 0.4$ s , $k_4 = 0.15768$ N/rpm [for (mps) = 6 m/s], $k_4 = 0.18448$ N/rpm [for (mps) = 7 m/s] and $k_2\, k_s = 0.18017115$ N/rpm [1]. The automatic speed control loop with $(PD)_1$ governor is shown in Figure (1). It is to be noted that the loop becomes unstable when eliminating k_d and raising k_p . Figure (2) shows the unstable Nyquist stability plot with p_1 governor, $k_p = 10$, $k_d = 0$ for the reference case 1 as indicated in Tables (1) and (2).

Table 1. Engine's varied parameters.

Case	bmp (atm).	mps (m/s)	λ	η_{vol}
1	10	6	1.15	0.92
2	10	6	1.15	0.95
3	10	6	1.35	0.92
4	10	6	1.35	0.95
5	10	7	1.15	0.92
6	10	7	1.15	0.95
7	10	7	1.35	0.92
8	10	7	1.35	0.95
9	12	6	1.15	0.92
10	12	6	1.15	0.95
11	12	6	1.35	0.92
12	12	6	1.35	0.95
13	12	7	1.15	0.92
14	12	7	1.15	0.95
15	12	7	1.35	0.92
16	12	7	1.35	0.95

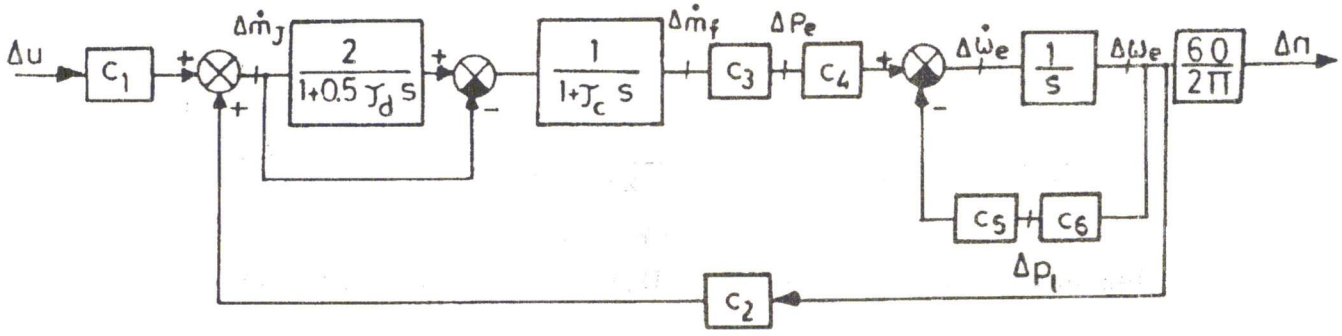

Figure 1. Block Diagram of Marine Diesel Engine.

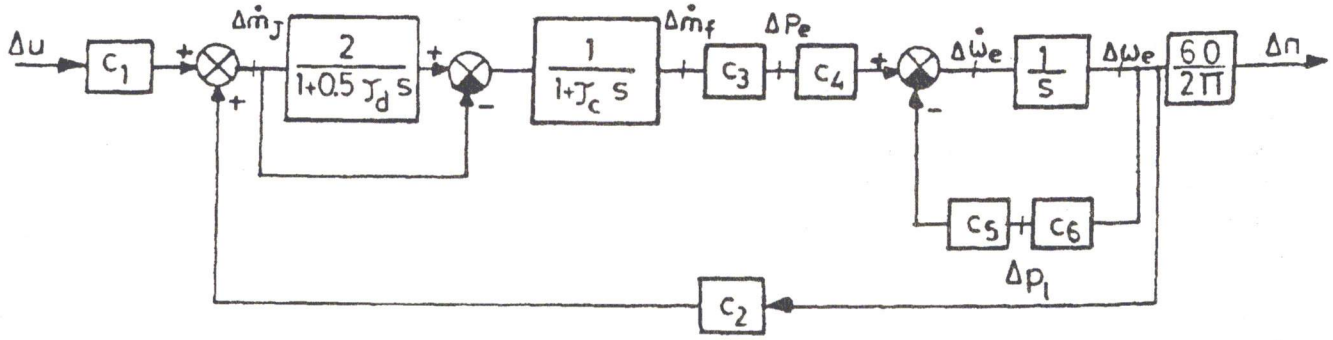

Figure 2. Block diagram of Marine Diesel Engine.

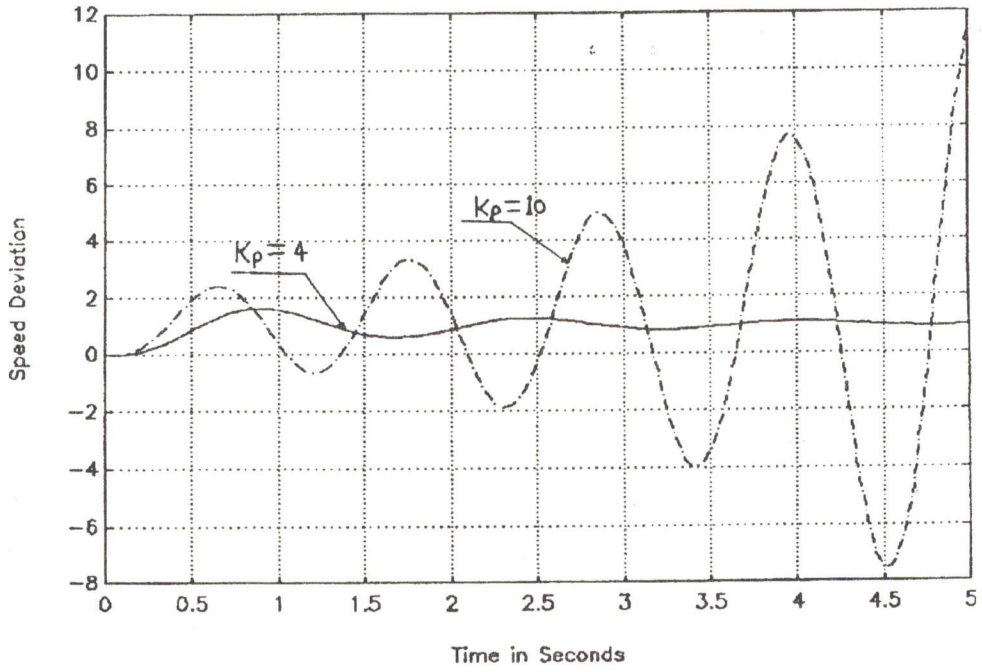

Figure 3. Transient response with (P1) governor, $K_p = 4,10$ $K_d = 0$, case 1.

Table 2. Coefficients of plant as control system.

Case	C_1, $\left(\frac{\text{Kg/s}}{\text{\% rack stroke}}\right)$	C_2 (kg)	$C_3^* 10^6$ Joule/kg)	$C^{4*} 10^6$ (S/kg.m^2)	$C_5^* 10^{-6}$ (S/kg.m^2)	$C_6^* 10^{-6}$ (Joule)	$\tau\omega c$ (sec)	τ_d (sec)
1	0.733	0.0554	15.2959	0.6685	1.137	1.494	0.1	0.05
2	0.7998	0.0573	14.7021	0.6685	1.137	1.494	0.1	0.05
3	0.6574	0.0471	17.984	0.6685	1.137	1.494	0.1	0.05
4	0.6782	0.0486	17.431	0.6685	1.137	1.494	0.1	0.05
5	0.902	0.0554	15.295	0.5726	0.9744	1.494	0.086	0.043
6	0.931	0.0572	14.812	0.5726	0.9744	1.494	0.086	0.043
7	0.7669	0.0471	17.4834	0.5726	0.9744	1.494	0.086	0.043
8	0.7912	0.0486	17.4316	0.5726	0.9744	1.494	0.086	0.05
9	0.7721	0.0553	18.375	0.6685	1.137	1.7924	0.1	0.05
10	0.7989	0.0572	17.7584	0.6685	1.137	1.7924	0.1	0.05
11	0.6574	0.0471	21.5826	0.6685	1.137	1.7924	0.1	0.05
12	0.681	0.0488	20.8347	0.6685	1.137	1.7924	0.1	0.05
13	0.901	0.0553	18.376	0.5726	0.9744	1.8252	0.086	0.043
14	0.832	0.0572	17.758	0.5726	0.9744	1.8252	0.086	0.043
15	0.7693	0.047	21.5127	0.5726	0.9744	1.8252	0.086	0.043
16	0.7939	0.0487	20.8479	0.5726	0.9744	1.8252	0.086	0.043

The Same phenomenon is display too in time domain as demonstrated in Figure (3). Moreover, a root locus graph is plotted in Figure (4) For case 1, k_p= 4, k_d= 0.5 s and k_1= 0:0.03: 1.5. Results obtained show that the zeros are located at + 40, -8, whereas the poles are located at- 39.598,-11.068 ,- 2.5 and - 1.033. Dynamic behaviour comparisons between cases 1 and 5-with the same governor w.r.t closed loop transient responses, open and closed loop frequency responses are indicated in Figures (5,6 and 7). Figure (8) illustrates the closed loop transient responses for cases 1 and 9 with the prementioned governor's constants. When varying the values of k_p and k_d to 10 and 1s respectively, the closed loop time and frequency responses for cases 1 & 5 and 1 &9 are portrayed in Figures (9-11) inclusive. In addition, Table (3) indicates relative stability comparisons when varying (mps), (bmp) and k_d.

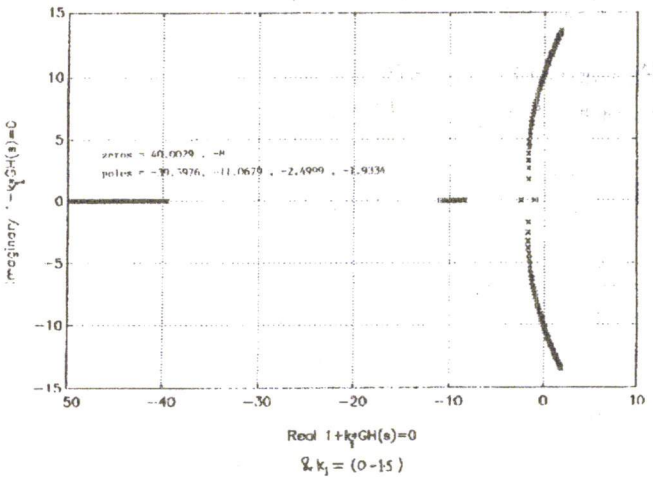

Figure 4. Root locus plot $(PD)_1$ governor K_p=4,K_d=0.5s, Referemce case 1.

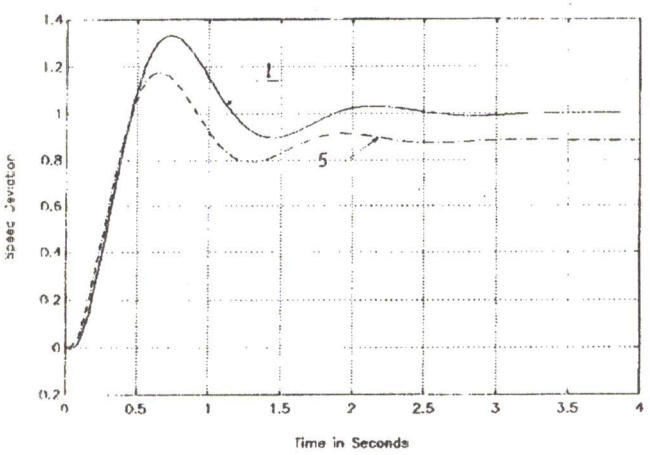

Figure 5. Transient response- $(PD)_1$ governor, K_p=4,K_d=0.5s cases 1&5.

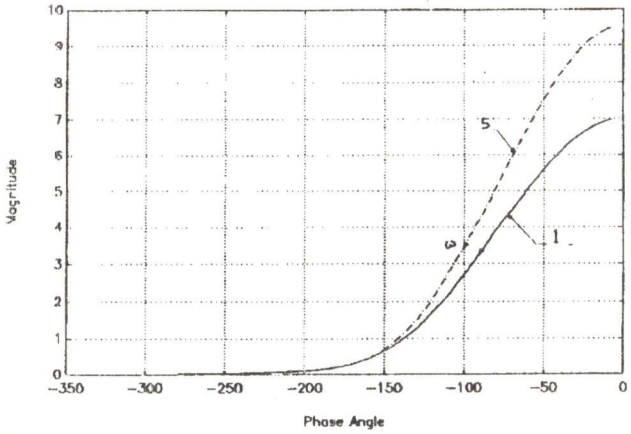

Figure 6. O.L. Mag-Phase plot with $(PD)_1$ governor, K_p=4,K_d=0.5s, cases 1&5.

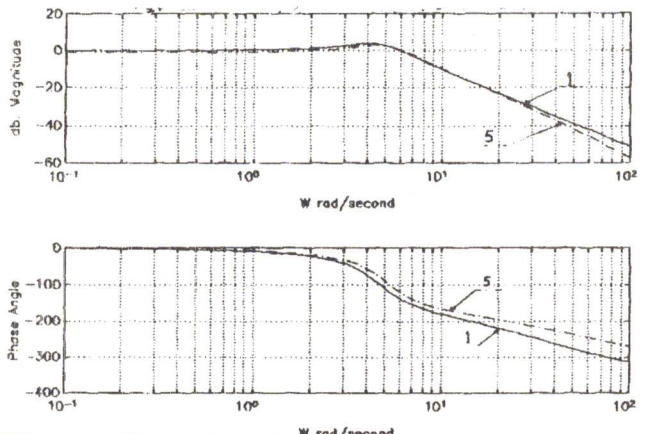

Figure 7. C.L. Bode plots-$(PD)_1$ governor, K_p=4,K_d=0.5s, cases 1&5.

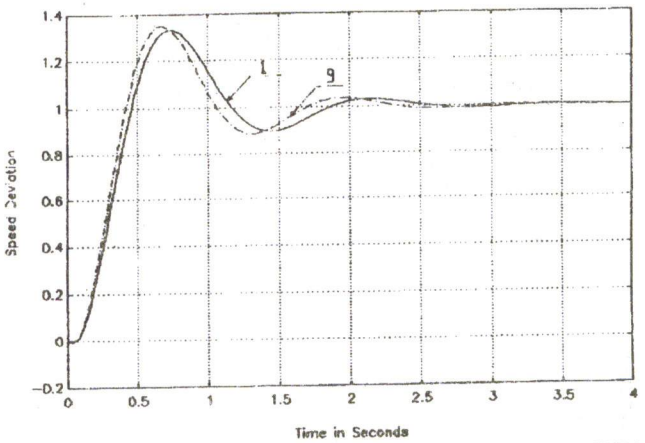

Figure 8. C.L. Transient responses - $(PD)_1$ governor, K_p=4, K_d=0.5s cases 1&9.

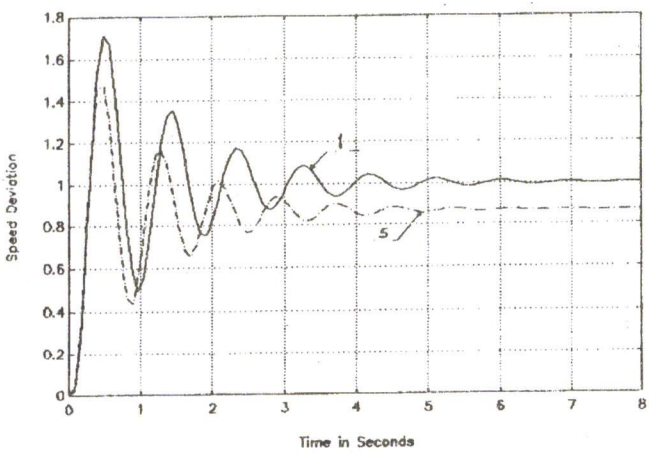

Figure 9. C.L. Transient responses with $(PD)_1$ governor, K_p=10, K_d=1s cases 1&5.

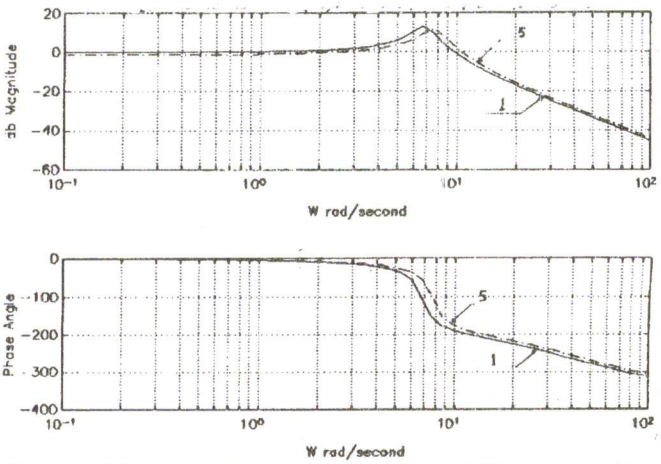

Figure 10. C.L. Bode plots with $(PD)_1$ governor, K_p=10, K_d=1s, cases 1&5.

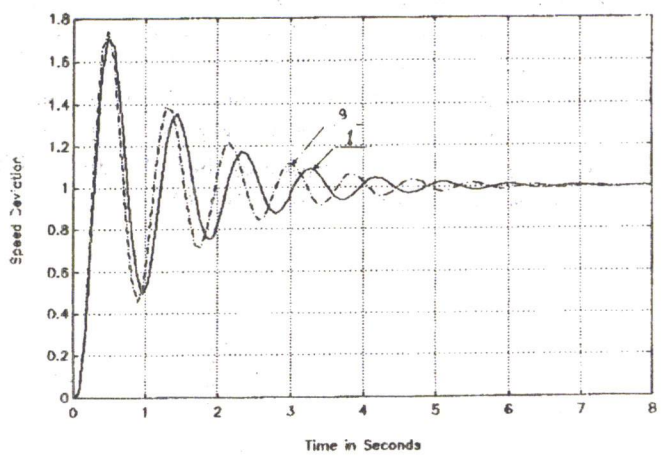

Figure 11. C.L. Transient responses - $(PD)_1$ governor, K_p=10, K_d=1s cases 1&9.

2- *Optimal Linear Quadratic Regulator Design by Reduced Matrix Riccati Equation.*

The quadratic performance index for optimal controller design minimizing a generalized state error Function [ξ(t)] - [X (t)] and imposing constraints on the control Vector - in order to compromise the control cost too- is given by [8,9]:

$$J = \int_{t=0}^{t=\tau_1} [\xi(t) - X(t)]^T Q[\xi(t) - X(t)]dt + \lambda_1 \int_{t=0}^{t=\tau_1} U^T(t) r_1 U(t)dt, \quad 0 \le t \le \tau_1 \qquad (1)$$

If the desired states ξ (t) are chosen as origin, the Lagrange multiplier λ_1 is included in r_1 matrix and letting $\tau_{1=\infty}$ the quadratic index becomes:

$$J = \int_0^{\infty} ([X]^T[Q][X] + [U]^T[r_1][U])dt \qquad (2)$$

The quadratic performance index for optimal controller design minimizing a generalized state error Function [ξ (t)] - [X (t)] and imposing constraints on the control Vector - in order to compromise the control cost too- is given by [8,9]:

Table 3. Relative stability with P_1 and $(PD)_1$ Governors w.r.t. Disturbance signal (y_o=6, τ=0.4 s).

Constants	Case	G_m	P_m	ω_π	ω_1
k_p=4	1	1.8931	29.8777	4.5216	3.316
k_p=4,k_d=0.5	1	15.9075	54.4729	42.1775	9.9377
k_p=4,k_d=1	1	3.0648	28.0833	26.9774	15.3581
k_p=4,k_d=2	1	1.1963	4.6652	24.1644	22.173
k_p=10, K_D=1	5	2.7885	26.7885	27.9423	16.6452
k_p=4,k_d=1	9	2.6435	23.6999	27.3104	16.9812

This concept when being applied to the system matrix equations [8,9], yields the matrix Riccati equation for proportional linear quadratic regulator's design namely:

$$\left.\begin{aligned} &[A]^T[P] + [P][A] - [P][B][r_1]^{-1}[B]^T[P] + [Q] = [O] \\ &\text{where } -[\alpha] = -[r_1]^{-1}[B]^T[P] \end{aligned}\right] \qquad (3)$$

where [Q] is a positive- definite (or positive semi-definite) real symmetric matrix and $[r_1]$ is a positive-definite real symmetric matrix .

Since the system has single input variable , the matrix [r_1] should be here a scalar quantity .

The matrix [P] which should be positive- definite real symmetric matrix is deduced from the solution of equation (3) and is used to find the optimal proportional state feedback for the regulator [8,9] .

Testing of positive-definiteness of matrices could be performed by Sylvester's theorem [8]

It. is apparent that the Diesel engine plant is controllable since the test matrix

$$[[B]\ [A]\ [B]\ [A]^2\ [B]] \qquad (4)$$

has a rank = 3 for all values of the parameters shown in Table (2). The concept of controllability involves the dependence of the state variables of the system on the inputs. It is essential to certify before designing a controller .

Refering to Figure (12-a) it could be written:

$$\left.\begin{aligned}
&\frac{X_1}{z_1} = \frac{C_3C_4}{C_5C_6 + s}\text{.....,}\\
&\frac{z_1}{X_2} = 1 - 0.5\,\tau_d\,.\,s\text{....,}\\
&\frac{X_2}{X_3} = \frac{1}{1 + 0.5\,\tau_d\,s}\text{.....,}\\
&\frac{X_3}{\Delta\dot{m}_j} = \frac{1}{1 + \tau_c\,s}\text{.....,}\\
&\Delta\dot{m}_j = C_1\,.\,\Delta u + C_2X_1 \quad \textit{and}\\
&\Delta n = 9.55\,X_1
\end{aligned}\right\} \qquad (5)$$

Equations (5) can be put in matrix form or:

$$\begin{bmatrix}\dot{X}_1\\ \dot{X}_2\\ \dot{X}_3\end{bmatrix} = \begin{bmatrix}-C_5C_6 & 2C_3C_4 & -C_3C_4\\ 0 & \frac{-1}{0.5\tau_d} & \frac{1}{0.5\tau_d}\\ \frac{C_2}{\tau_c} & 0 & \frac{-1}{\tau_c}\end{bmatrix}\begin{bmatrix}X_1\\ X_2\\ X_3\end{bmatrix} + \begin{bmatrix}0\\ 0\\ \frac{C_1}{\tau_c}\end{bmatrix}.\Delta u \qquad (6)$$

and

$$\Delta n = [\,9.55\ 0\ 0\,]\,[\,X1\ \ X2\ X3]T \qquad (7)$$

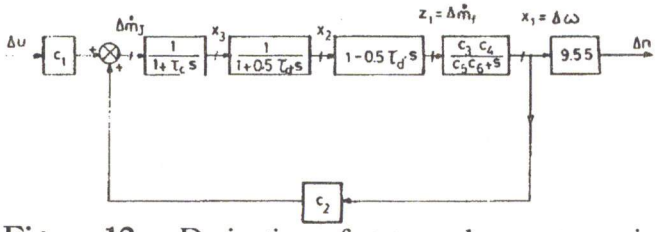

Figure 12-a. Derivation of state and output matrix equations of the marine diesel plant.

Substituting the particular values of the reference case number 1 in equations (6,7) and selecting r_1=1 and [Q]=90 [I], equations (3) yield:

$$\left.\begin{aligned}
&[P] = \begin{bmatrix}12.759 & 5.289 & 0.893\\ 5.285 & 3.386 & 0.768\\ 0.893 & 0.768 & 1.335\end{bmatrix}\text{.....,}\\
&-[\alpha] = [-6.902\ -5.938\ -10.319]\ \textit{and}\\
&[a] = [A] - [B].[\alpha]
\end{aligned}\right\} \qquad (8)$$

Figure (12-b) represents the closed loop block diagram for optimal linear quadratic regulator design. In order to indicate the effect of changes in (mps) and (bmp), digital computations for cases 1 & 5 and 1 & 9 in time and frequency domains for closed and open loops are shown in figures from (13) to (18) inclusive, while comparisons of their relative stability measures are tabulated in Table (4).

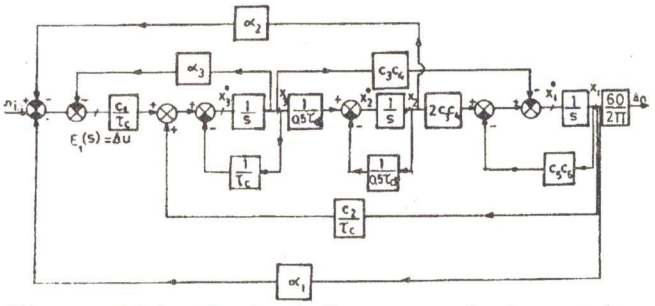

Figure 12-b. Optimal linear quadratic regulator design by riccati method.

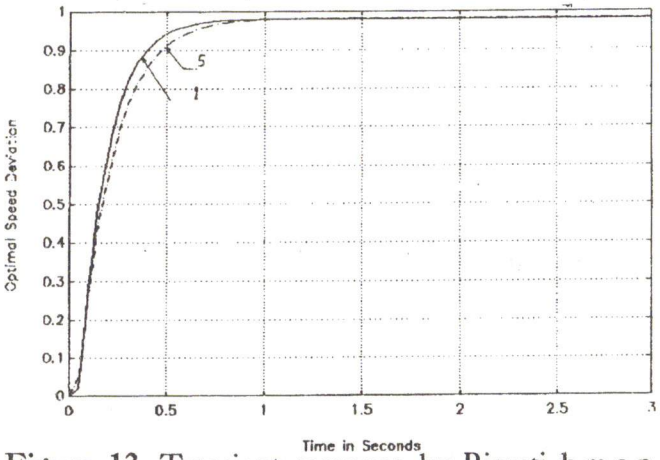

Figure 13. Transient response by Riccati b.m.e.p. =10, λ=1.15, η_{vol}=0.92.

It is worthmentioing that the open loop transfer function for Riccati solution can be deduced from figure (12-b) namely:

Table 4. Relative stability measures with optimal linear quadratic regulator.

Case	G_m	P_m	ω_π	ω_1
1	4.5729	83.0061	28.2855	6.8037
5	6.001	89.295	33.4238	6.0383
9	3.8332	78.8734	28.8786	8.1665

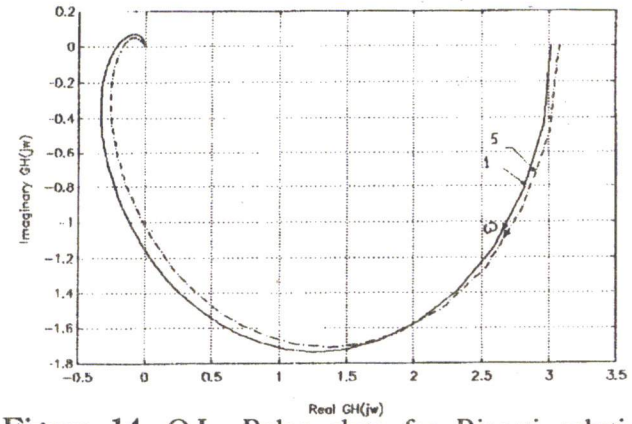

Figure 14. O.L. Polar plots for Riccati solution b.m.p.=10, λ=1.15, η_{vol}=0.92.

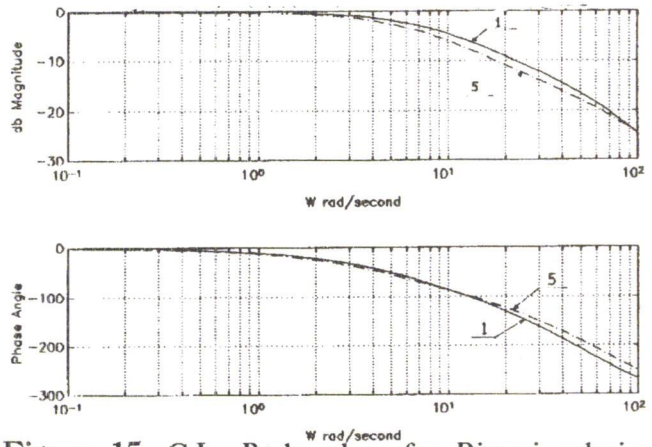

Figure 15. C.L. Bode plots for Riccati solution b.m.p.=10,λ=1.15, η_{vol}=0.92.

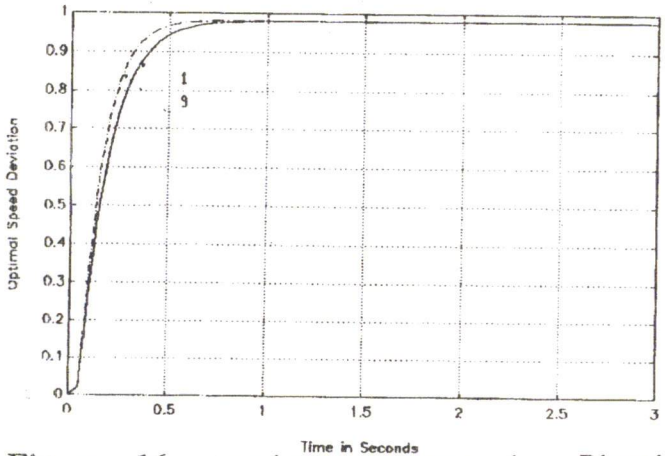

Figure 16. transient response by Riccati m.m.s=6,λ=1.15, η_{vol}=0.92.

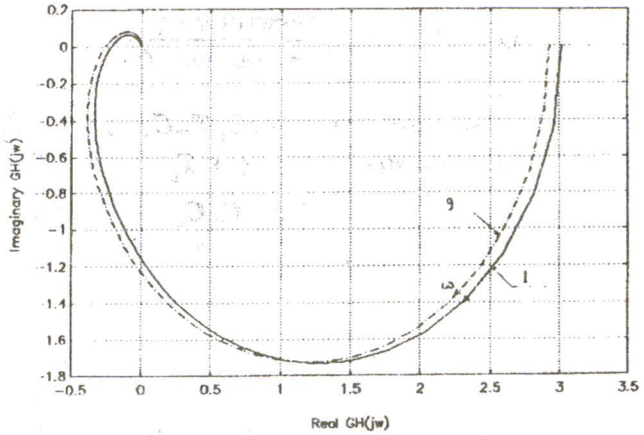

Figure 17. O.L. Polar plots for Riccati solution m.p.s.=6,λ=1.15, η_{vol}=0.92.

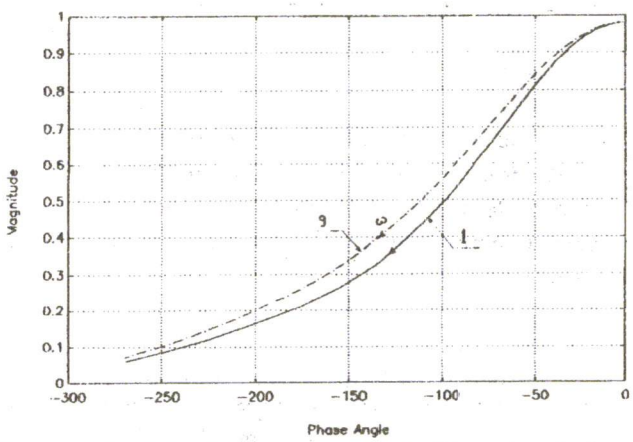

Figure 18. C.L. Mag-Phase angle-Riccati solution, m.p.s.=6,λ=1.15, η_{vol}=0.92.

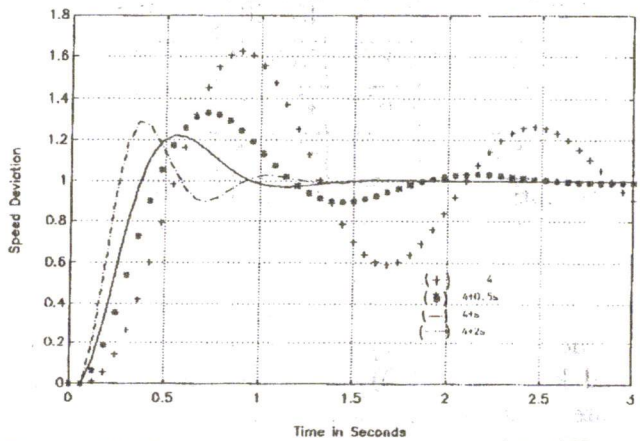

Figure 19. Various transient responses with different governors, case 1.

$$O.\ L.\ T.\ F = \frac{Numerator\ (s)}{Denumerator\ (s)}$$

Where

$$Numerator\ (s) = (2*C_1.T_C.C_3.C_4.T_d - C_1.T_C.C_3.C_4.T_d)\ \alpha_1 - C_1.C_3.C_4.T_C.\alpha_1.s$$

$$Denumerator\ (s) = (s + T_c) * (s + T_d)\ (s + C_5C_6) + \alpha_3 . C_1.T_c * (s + T_d) * (s + C_5.C_6) - 2C_1.C_3.C_2.C_4.T_d.T_c^2 + C_1.C_3.C_2.C_4.T_c^2 * (s + T_d) + T_d.\alpha_2.C_1T_c.\ (s + C_5.C_6)\ ,$$

$$T_c = \frac{1}{\tau_c} \quad and \quad T_d = \frac{1}{(0.5\ \tau_d)} \qquad (9)$$

Likewise, for the sake of the determination of the influence of the proportional and derivative gains k_p and k_d of the $(PD)_1$ controller versus the optimal state feedback regulator on the control loop of Diesel engine when operating with the reference plant (case 1), extensive computations in time and frequency domains for both closed and open loops are displayed in Figures from (19) to (24) inclusive, bearing in mind that the P_1 speed controller with k_p=10 does not realize the absolute stability with the plant. Besides, Table (5) summarizes the indicators of the degree of stability for the reference plant (case 1) when operating with P_1, $(PD)_1$ and optimal controllers.

Table 5. Degree of stability indicators for case (I) with P_1, $(PD)_1$ and optimal controllers.

Controller	G_m	P_m	ω_π	ω_1
10 (unstable)	0.6988	-13.408	4.9361	6.-163
4	1.704	20.4371	4.9793	3.7072
10 + s	1.7432	13.6402	8.9053	6.5782
4 + 2 s	2.8712	53.3851	15.2039	7.3496
4 + s	4.6278	47.1072	13.5551	4.7185
4 + 0.5 s	4.9697	42.3209	10.2192	3.9557
Riccati	4.5729	83.0061	28.2855	6.8037

Likewise, for the sake of the determination of the influence of the proportional and derivative gains k_p and k_d of the $(PD)_1$ controller versus the optimal state feedback regulator on the control loop of Diesel engine when operating with the reference plant (case 1), extensive computations in time and frequency domains for both closed and open loops are displayed in figures from (19) to (24) inclusive, bearing in mind that the P_1 speed controller with k_p=10 does not realize the absolute stability with the plant. Besides, Table (5) summarizes the indicators of the degree of stability for the reference plant (case 1) when operating with P_1, $(PD)_1$ and optimal controllers.

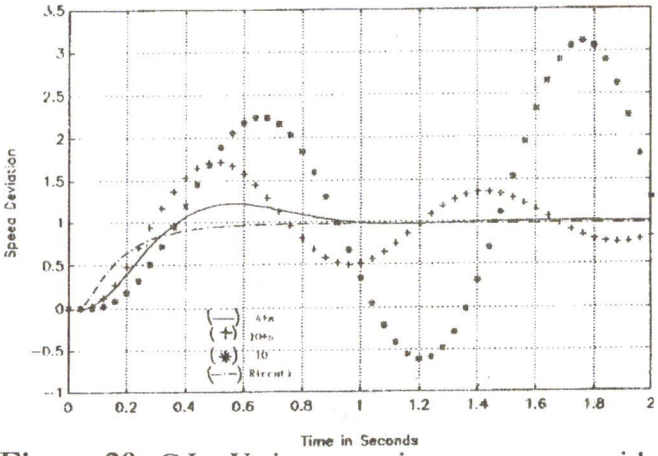

Figure 20. C.L. Various transient responses with different governors, case 1.

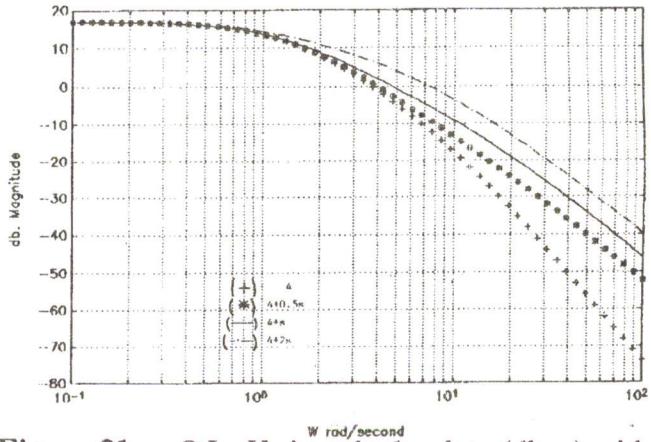

Figure 21-a. O.L. Various bode plots (db-w) with different governors case 1.

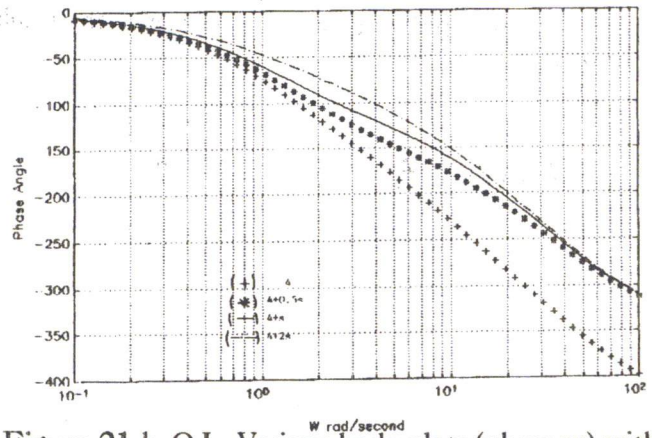

Figure 21-b. O.L. Various bode plots (phase-w) with different governors case 1.

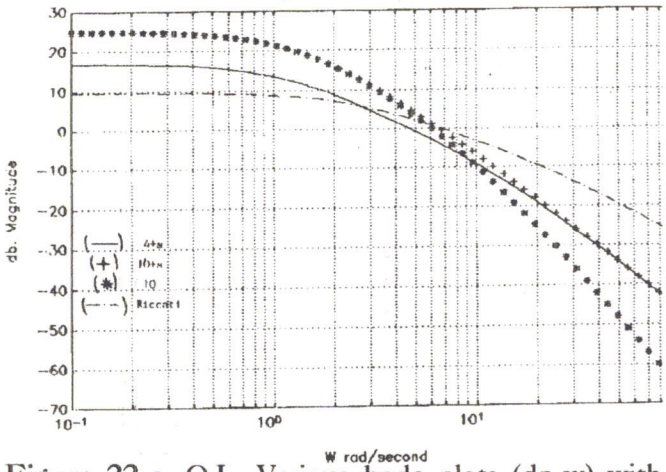

Figure 22-a. O.L. Various bode plots (dp-w) with different governors case 1.

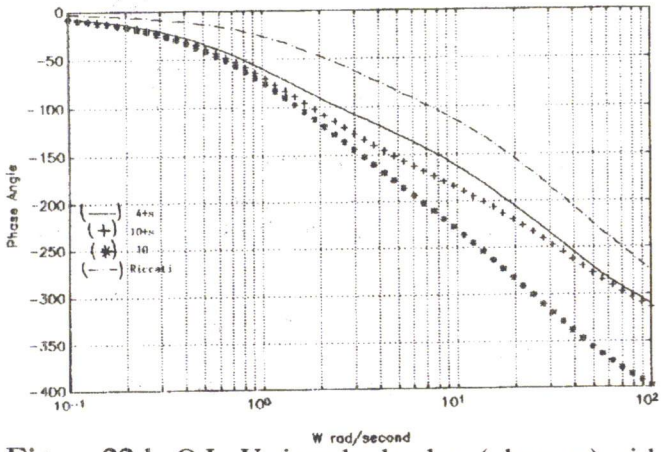

Figure 22-b. O.L. Various bode plots (phase-w) with different governors case 1.

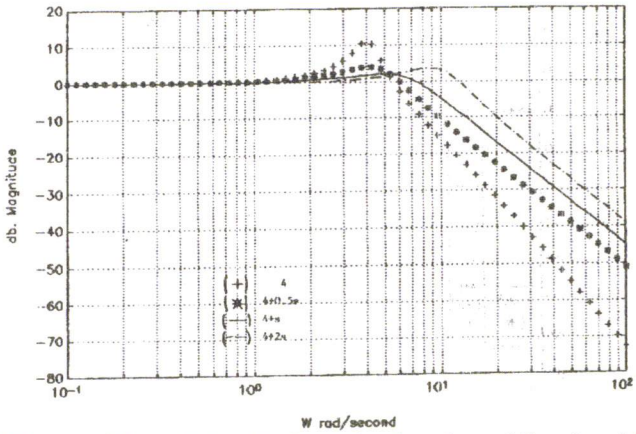

Figure 23-a. C.L. Various bode plots (db-w) with different governors case 1.

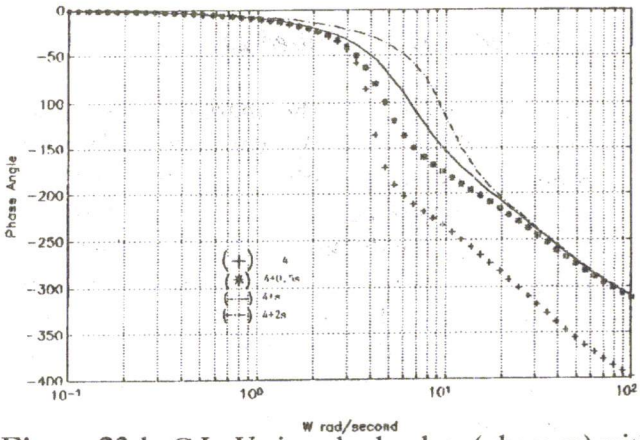

Figure 23-b. C.L. Various bode plots (phase-w) with different governors case 1.

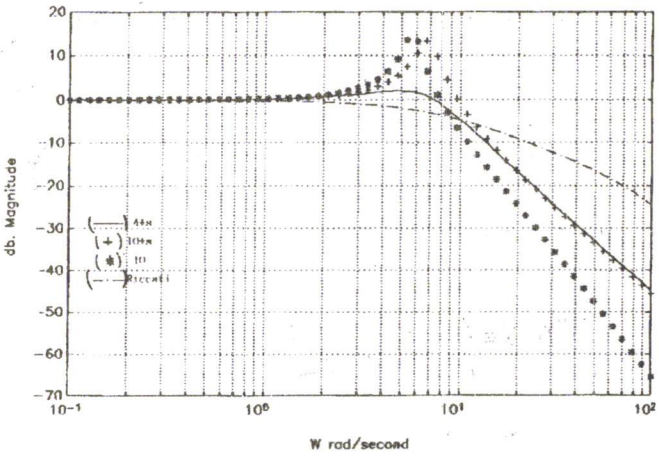

Figure 24-a. C.L. Various bode plots (dp-w) with different governors case 1.

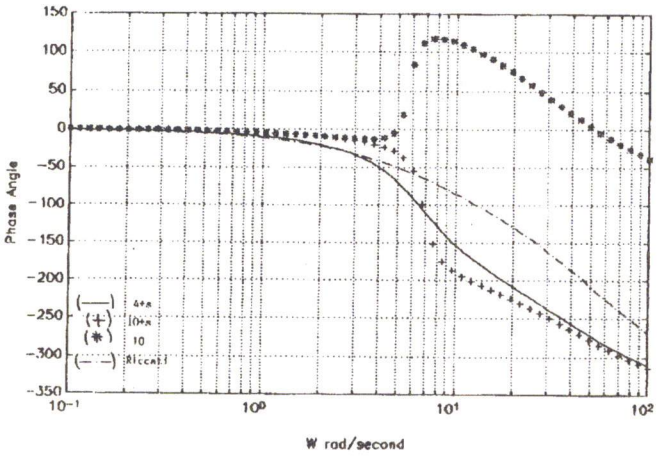

Figure 24-b. C.L. Various bode plots (phase-w) with different governors case 1.

3- *Regulation with optimized gain $(PI)_0$ controller*

The speed control of the marine Diesel engine is investigated with $(PI)_0$ controller. An arbitrary proposal is assumed with $k_p = 4$ and $k_I = 5\ s^{-1}$, then a parameter-optimized solution is tried to find the value of k_1 (with kp= 4 - the basic gain for proportional control action) based on the integral of the squares of the error optimization index and Parseval's equation. While the controller is considered to be ideal thus omitting the time delay τ, the values of k_4 and $k_2.k_S$ still hold good. Figure (25) illustrates the block diagram of the automatic speed control loop isochronously by $(PI)_0$ speed governor. Despite that the strict fixation of speed of marine propulsion Diesel engines with load variation is not essential as being the case with Diesel generators, this case study will be analyzed for scientific comparison.

According to the ISE performance index the frequency - time correlation derived from Fourier integrals [8], it could be written :

$$\int_0^\infty e_1^2(t)dt \equiv \int_0^\infty e_1(t)\left(\frac{1}{2\pi j}\int_{\sigma-j\infty}^{\sigma+j\infty} E_1(s).e^{+st}ds\right)dt$$

Provided that :

$$\int_0^\infty |e_1(t)|dt < \infty$$

Interchanging the order of integration in equation (10) and applying the definition of Laplace transforms then:

$$\int_0^\infty e_1^2(t)\,dt \equiv \frac{1}{2\pi j}\int_{\sigma-j\infty}^{\sigma+j\infty} E_1(s)\left(\int_{t=0}^{t=\infty} e_1(t)e_1^{st}dt\right)ds = \underbrace{\frac{1}{2\pi J}\int_{-J\infty} E_1(-s)ds}_{J\infty} \quad (11)$$

Jury [6,7] computed and published Tables for the solution of equation (11) provided that $E_1(s)$ can be written in the form :

$$E_1(s) = \frac{\text{Num}(s)}{\text{Den}(s)} \text{ where}$$

$$\text{Num}(s) = b_o + b_1.s + \ldots\ldots\ldots + b_{n-1}.s^{n-1},$$

$$\text{Den}(s) = a_o + a_1.s + \ldots\ldots\ldots + a_{n-1}.s^{n-1},$$

Where Den (s) has zeros only in the left half side of the complex plane.
The result for n=3 and n = 4 for continuous systems are as follows [6,7,8] :

$$J_3 = \frac{b_2^2.a_0a_1 + a_0a_3(b_1^2 - 2b_0.b_2) + b_0^2.a_2a_3}{2a_0.a_3(-a_0.a_3 + a_1.a_2)} \quad (12)$$

$$\text{and } J_4 = \frac{b_3^2(-a_0^2.a_3 + a_0.a_1.a_2) = a_0.a_1.a_4(b_2^2 - 2b_1.b_3) + a_0.a_3.a_4(b_1^2 - 2b_0.b_2)}{2a_0a_4(-a_0.a_3^2 - a_1^2 + a_1.a_2.a_3)} + \frac{b_0^2(-a_1.a_4^2 + a_2.a_3.a_4)}{2a_0a_4(-a_0.a_3^2 - a_1^2 + a_1.a_2.a_3)} \quad (13)$$

Application of equation (13) to $E_1(s)$ derived from Figure (25) for case 1, k_p=4, y_o=6, k_4 = 0.15768 (N/rpm) and k_2k_s= 0.18017115 (N/rpm), it follows :

$$\frac{dJ_4}{dk_1} = 9.0705k_1^4 + 2.1536*10^4k_1^3 + 6.8707*10^7k_1^2 - 2.8079*10^9k_1 + 4.2092*10^9 = 0 \quad (14)$$

Solution of equation (14) yields two refused conjugate complex roots beside k_I= 1.6 and 38.8 s^{-1}.

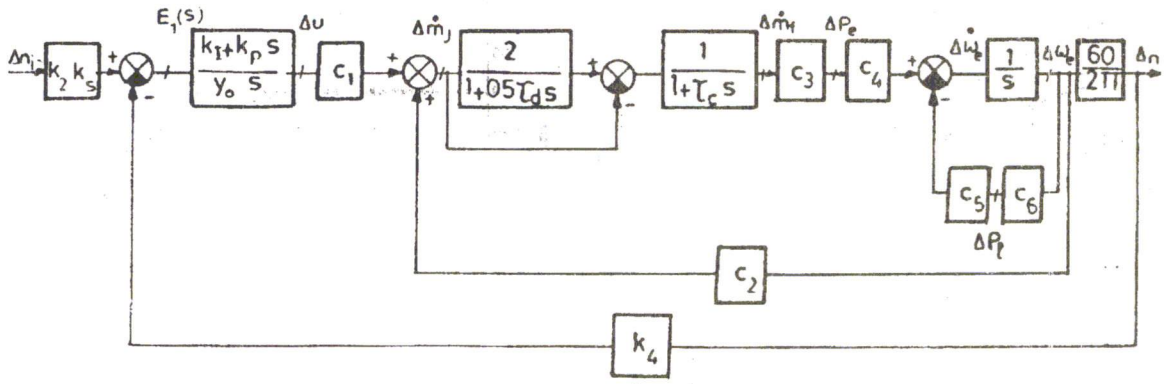

Figure 25. Speed control with proportional plus integral controller.

Figures (26, 27), and (28) display the closed loop transient responses, open loop and closed loop Bode plots respectively, for case 1 with k_I= 5, 1.6 and 38.8 s^{-1} ; the latter value of k_I gives an unstable solution with the other chosen values of parameters. In addition, Table (6) summarizes the values of gain and phase margins, phase and gain cross-over frequencies. Since the whole transient duration approaches only one second, further comparisons between cases 1,5 and 9 seem to be of minor significance .

Table 6. Relative stability measure for Case (1) with $(PI)_o$ controller.

Governor	G_m	P_m	ω_π	ω_1
$\frac{4s+5}{6s}$	3.114	40.1767	13.7112	6.3455
$\frac{4s+1.6}{6s}$	3.2811	48.431	14.4776	6..2535
$\frac{4s+38.8}{6s}$ (unstable)	0.564	-13.7547	4.5263	8.5806

4- *Regulation with optimized gain (PDF) control*

One of the most recent algorithms in control strategy is Pseudo derivative feedback (PDF), a new control structure that captures the advantages of derivative (D) action without the attendant difficulties caused by a differentiator located in the forward path of the controller [3,4]. This concept developed by Phelon of Cornell university eliminates all the numerator dynamics in the command input transfer function. For a second or higher order plant, only the integral controller is located in the forward path while the feedback path transfer function has the from: $(1 + k_{D1}.s + k_{D2}.s^2)$ in order that the control signal depends on the output , its derivatives and its integral. Since reliable second order derivatives of signals are almost impossible to obtain, the problem is overridden by adopting only proportional-derivative action in a feedback path as a minor loop. Ideal integral (τ=o) and proportional derivative control actions are concerned as indicated in Figure (29). The principle of parameter optimization will be applied to both k_p and k_d.

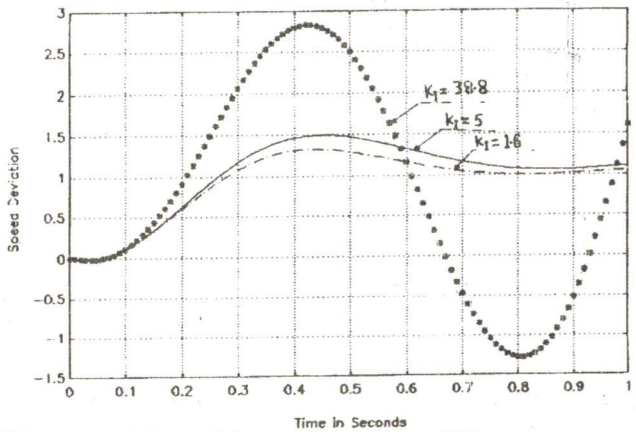

Figure 26. C.L. Responses-$(PI)_o$ governor, k_p=4,k_I=5,1.6,38.8 case 1.

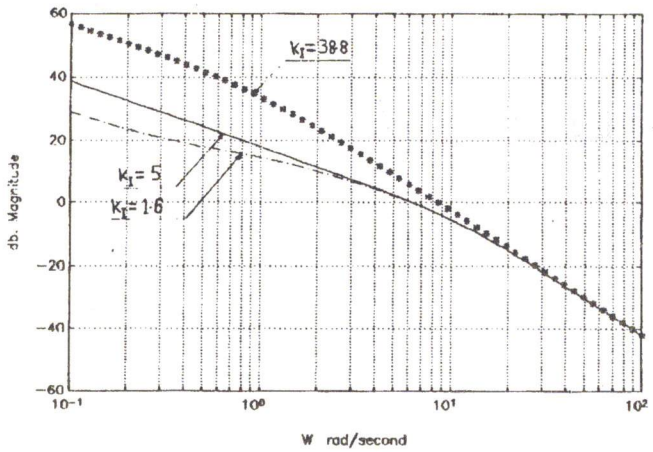

Figure 27-a. OL. Bode plots (dp-w) $(PI)_o$ governors, k_p=4,k_I=5,1.6,38.8 s^-1, case 1.

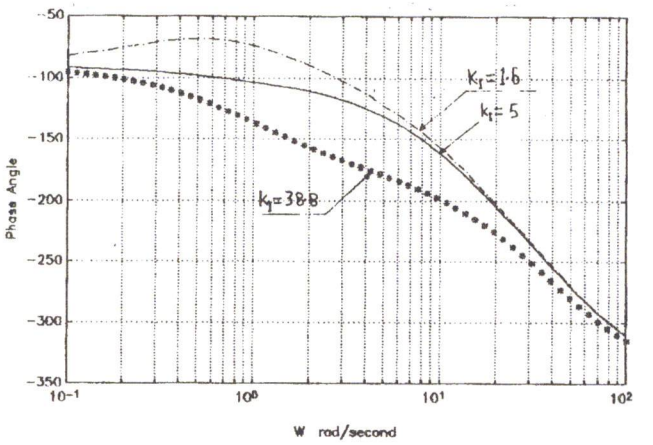

Figure 27-b. OL. Bode plots (Ph-w) $(PI)_o$ governors, k_p=4,k_I=5,1.6,38.8 s^-1, case 1.

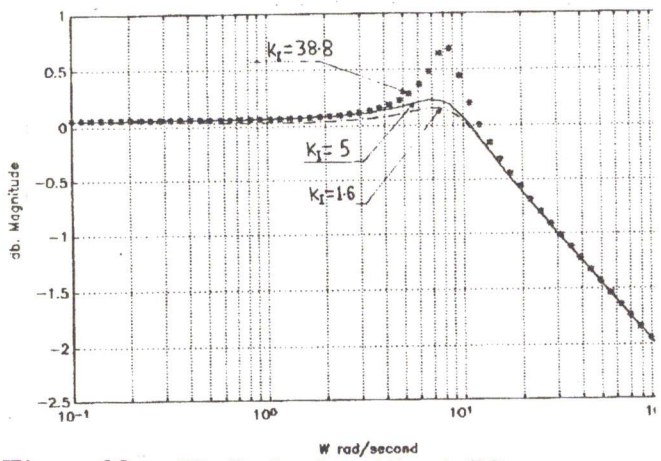

Figure 28-a. CL. Bode plots (db-w) $(PI)_o$ governors, k_p=4,k_I=5,1.6,38.8 s^-1, case 1.

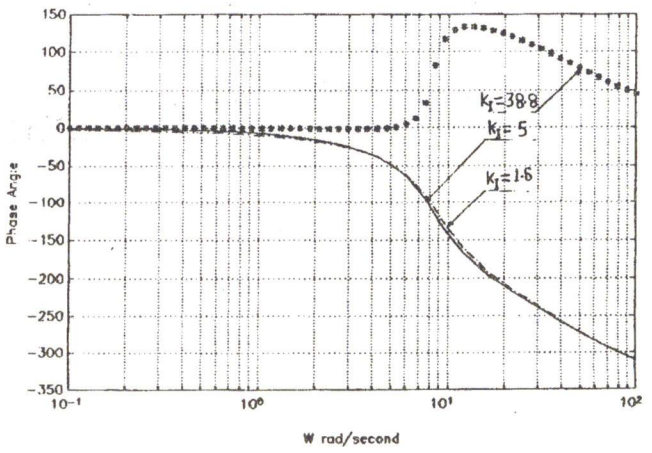

Figure 28-b. CL. Bode plots (db-w) $(PI)_o$ governors, k_p=4,k_I=5,1.6,38.8 s^-1, case 1.

Considering the numerical values of the reference plant of case 1 (Tables (1) and (2)) and selecting the adequate value of k_I= 1.6 s^{-1} - which was obtained from parameter optimization in section 3- while keeping the values of k_4= 0.15768 N/rpm and $k_2.k_s$= 0.18017115 N/rpm, the error signal $E_1(s)$ of the block diagram shown in Figure (29) becomes :

$$\left.\begin{aligned} E_1(s) &= \frac{1.0806869 D_1(s)}{6D_1(s).s + N_1(s).(1.6k_d.s + 1.6k_p + 0.25228)} \\ &\text{Where } N_1(s) + -1.88698*s + 75.4848 \text{ and} \\ D_1(s) &= 0.0025*s^3 + 0.129246*s^2 + 1.225649*s + 1.13219 \end{aligned}\right\} \quad (15)$$

Substitution from equation (15) into equation (13) and setting values for either k_p or k_d in the two resulting equations namely:

$$\left.\begin{aligned} \frac{\partial J_4(k_p, k_d)}{\partial k_p} &= 0 \text{ and} \\ \frac{\partial J_4(k_p, k_d)}{\partial k_d} &= 0 \end{aligned}\right\} \quad (16)$$

the solutions indicated in Table (7) are obtained. Figures (30-a &b) represent comparisons between closed loop transient responses for the stable cases shown in Table (7).

Table 7. Regulation with (PDF) control-case (1). optimized values of k_p or k_d and absolute stability of the loop.

k_p(-)	k_d (s)	Roots of closed loop	Absolute stability
0.0115	1	-49.305,-1.1166±13.0244j, -0.1617	stable
0.0136	0.5	-45.2347,-0.3189,-3.0724±9.2831j	stable
0.4834	0.5	-45.1379,-1.3155,-2.6225±8.9473j	stable
3	1	-49.1629,1.1255,-0.705±12.7508j	stable
1.9678	0.700645	-55.282,-1.0635,+2.258±13.582j	unstable
1.9678	2	-55.282,-1.0635,+2.258±13.582j	unstable
4	0.77919-5	-46.9373,-6.0425,+0.6407±10.845j	unstable
6	0.900505	-47.5929,-7.483,+1.6888 ±11.06774j	unstable
8	0.994901	-48.0171,-8.6998,+2.5092±12.2858j	unstable

imposed constrained values

$k_1 = 1.6\ s^{-1}$
$k_4 = 0.5768$ N/rpm
$k_2\ k_5 = 0.18017115$ N/rpm

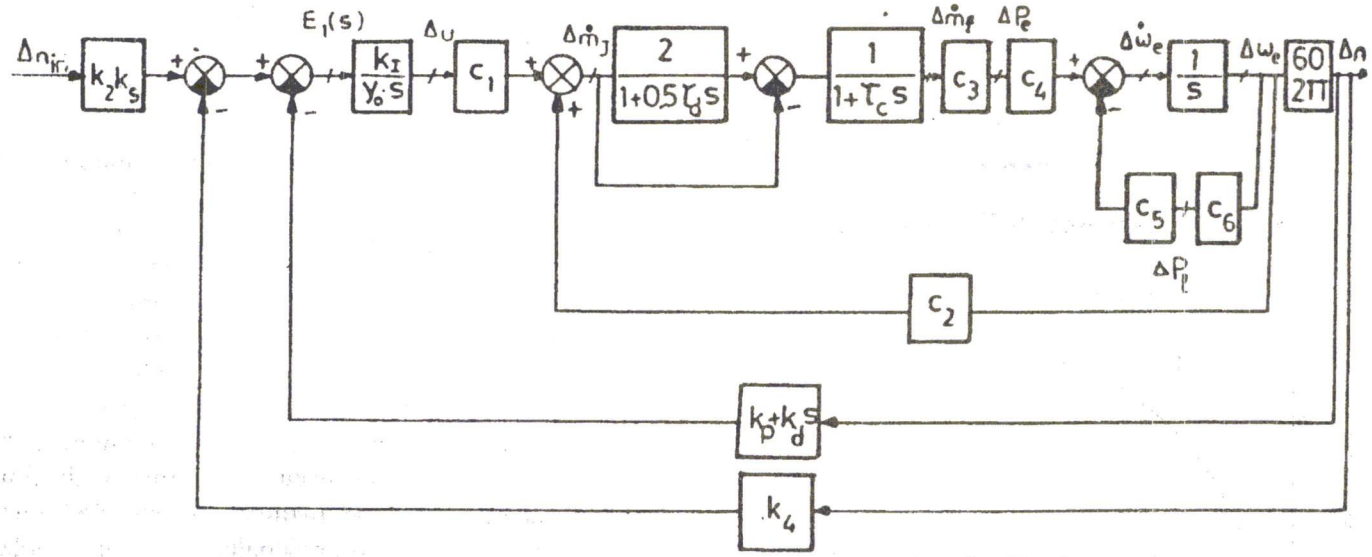

Figure 29. Speed regulation with pseudo derivative feedback.

It is evident that values of k_p= 0.0136, k_d= 0.5 s and k_I= 1.6 s^{-1} express an optimized acceptable dynamic performance from the point of view of pole-zero mapping, absence of oscillations and non excessive settling time. Besides, an acceptable final value w.r.t the command signal ($\Delta n\ (\infty) = 1.05$) is obtained with the aforementioned selected values for the gains k_p, k_I and k_d where:

$$\Delta n(\infty) = \lim_{t\to\infty}\left[\sum_{i=1}^{m}\frac{1}{(m-1)!}\left(\lim_{s\to s_1}\left(\frac{d^{m-1}}{ds^{m-1}}\Delta n(s).e^{+st}.(s-s_i)^m\right)\right)\right] \quad (17)$$

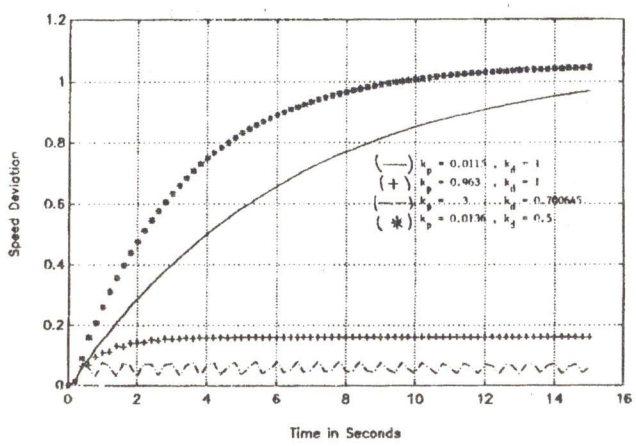

Figure 30-a. Responses -(PDF) governors, case 1.

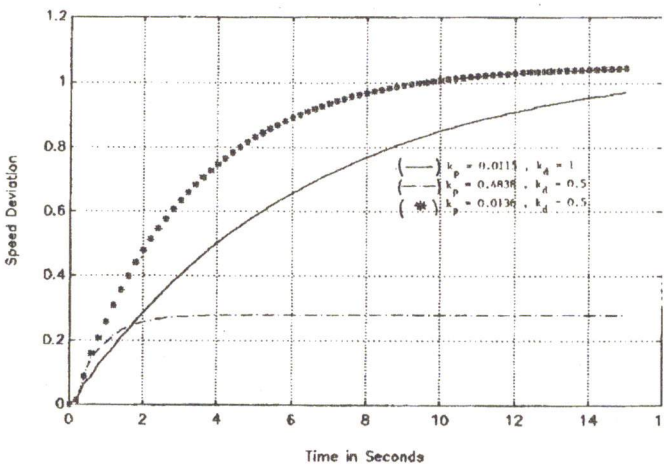

Figure 30-b. Responses -(PDF) governors, case 1.

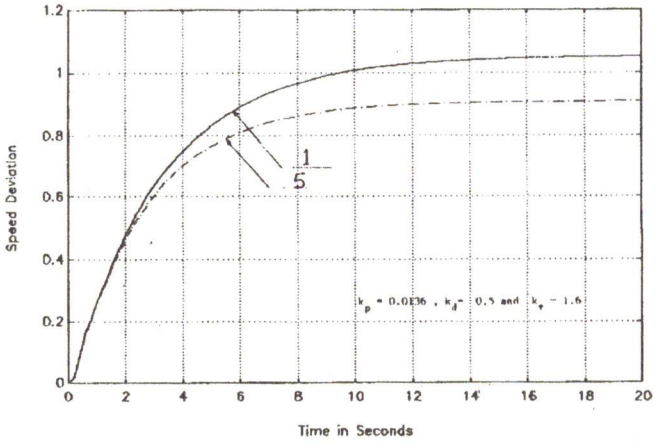

Figure 31. C.L. Transient responses, cases 1&5, with (PDF) governor.

The closed loop transient responses and Bode Plots for cases 1 and 5 are displayed in Figures (31,32) while the closed loop transient responses beside the open loop Nyquist plots for cases 1 and 9 are demonstrated in Figures (33, 34) respectively. Moreover a relative stability analysis with (PDF) speed controller is presented in Table (8).

Table 8. Relative stability with (PDF) controller with $k_1 = 1.6\ s^{-1}$

Gains	Case	G_m	P_m	ω_π	ω_1
k_p=0.0136, k_d=0.5	1	2.6014	39.5127	14.5268	7.5376
k_p=0.4834, k_d=0.5	1	2.4476	34.4722	13.5317	7.422
k_p=0.4834, k_d=0.5	5	2.8787	41.922	16.4581	7.9311
k_p=0.4834, k_d=0.5	5	2.6826	36.3333	15.7229	8,0973
k_p=0.4834, k_d=0.5	9	2.3367	35.3164	15.0511	8.5283
k_p=0.4834, k_d=0.5	9	2.1044	29.7938	13.9456	8.5387

5- *Regulation with optimized gain (PMD) control.*

The establishment of control engineering technology in what concerns the fundamental principles for the determination of conventional controllers properties and specifications to suit a regulating system for a specified plant has urged researchers to develop new techniques and control algorithms whose merits overweigh those of traditional controllers. Since the last years of the sixth decade, increasing attention was oriented to the analysis and study of control systems with time delays (dead time). The interest was extended too to the investigation of intentionally imposing a delay time to the controller. Suh and Bien [5] proposed the introduction of the proportional minus delay (PMD) control element located in the major feedback line and whose transfer function has the form: $1+(k_m/h_1)(1-e^{-h_1 s})$ which physically represents a pulse function followed after a time (h_1) by a reduced step function.

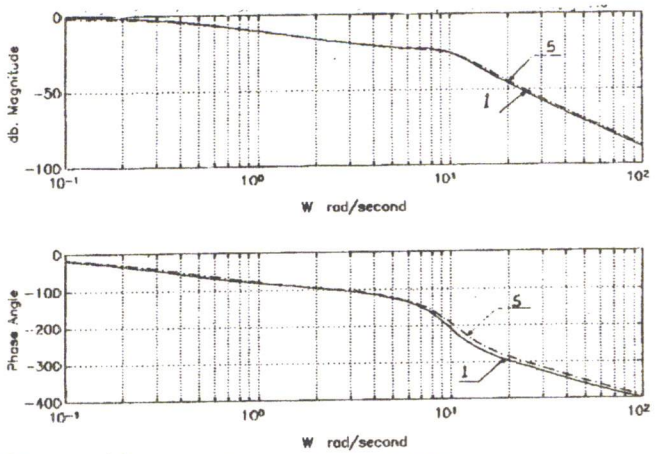

Figure 32. C.L. Bode plots (PDF) governor, cases 1&5, k_p=0.0136, k_d=0.5, K_I=1.6.

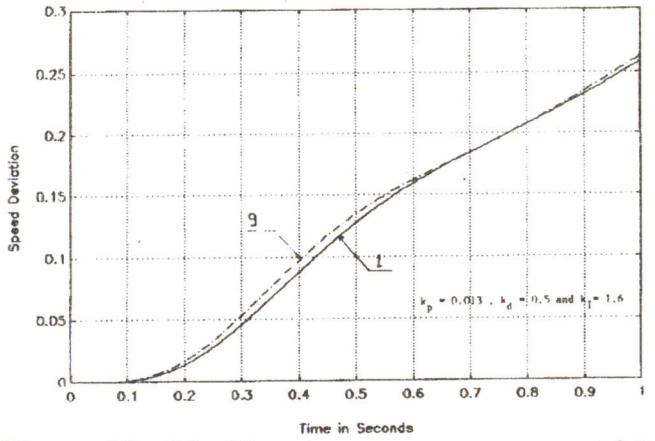

Figure 33. C.L. Transient responses, cases 1&9, with (PDF) governor.

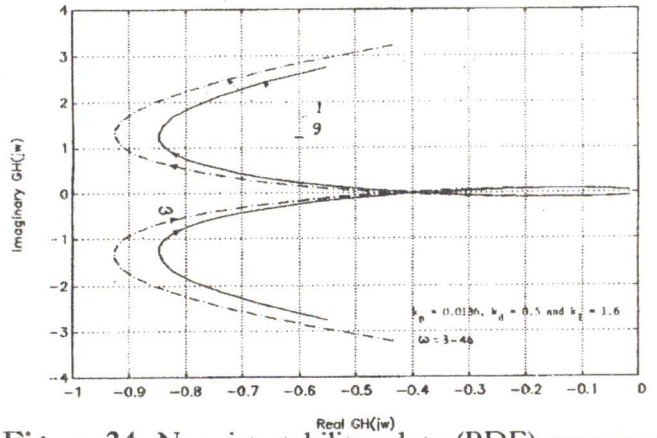

Figure 34. Nyquist stability plots (PDF) governor cases 1&9.

It is aimed here to investigate the behaviour of the marine Diesel engine with (PMD) control. In order to get the possibility to compare results obtained with (PDF) control, an additional I_o controller is placed in the forward path as shown in Figure (35-a), and the parameter-optimized concept will be applied. The plant is first simplified from $(PD)_3$ to $(PD)_2$, by omitting $\tau_{c\,c}$, while the (PMD) element is treated with Padé first approximation as illustrated in Figure (35-b). The reason is to utilize polynomials of the ISE indices got from Parseval's equation and tabulated in [6,7,8]. Data of case 1 Tables (1,2) is applied to the control loop shown in - figure (35-b) with h_1= 0.1 s and y_0= 6. Equation (13) is applied to the error signal E_1 (S) and setting values for k_I, the corresponding optimized values of k_m obtained from computer solutions [11,12] are listed in Table (9). The closed loop transient responses with the values of the gains k_I and k_m shown in Table (9) are displayed in - figure (36-a,b), whereas their closed loop Bode Plots are shown in figures (37-a,b). It is obvious that the most appropriate values of parameters are :

k_I= 0.288285 s^{-1}, k_m= 0.943849 s and h_1 = 0.1 s.

Table 9. Optimize Gains

$k_1(s^{-1})$	k_m (s) optimized	Absolute Stability
0.05 (optimized)	1.08357	stable
0.288285 (optimized)	0.943849	stable
1.6 (assumed)	0.536113	stable
5 (assumed)	0.364853	unstable
10 (assumed)	0.294853	unstable

Now these adequate values of the parameters of the (PMD) plus I_o controller are applied to the automatic speed control loop with the non- simplified $(PD)_3$ Diesel plant for cases 1, 5 and 9 to show how (mps) and (bmp) affect the dynamic performance of closed loop time and frequency responses and the degree of stability as shown in - figures (38-41) inclusive and Table (10).

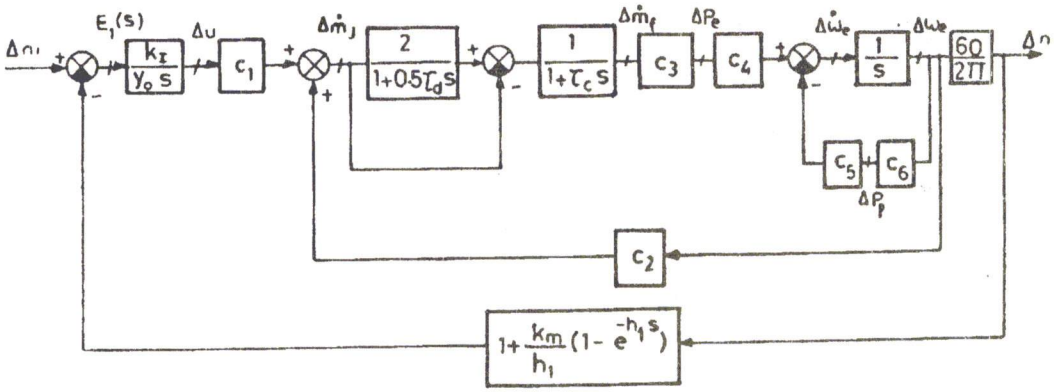

Figure 35-a. Speed regulation with proportional minus delay plus integral controller

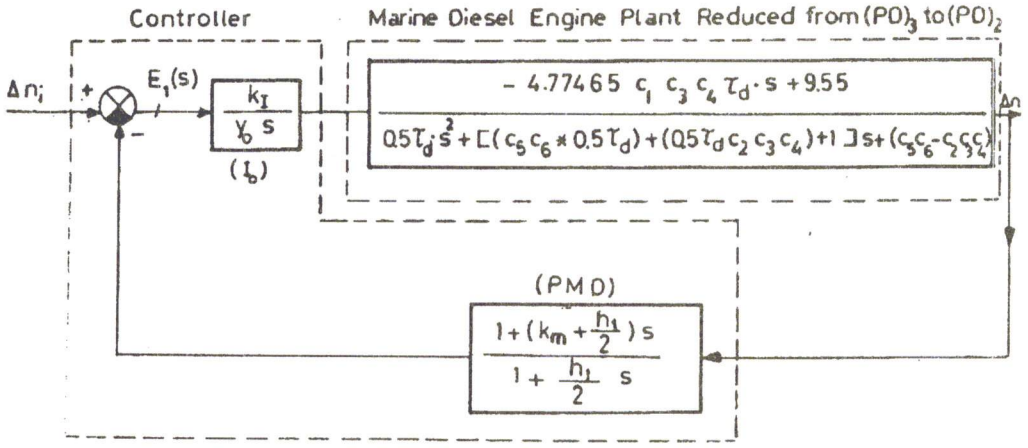

Figure 35-b. Simplified block diagram of that shown in Figure (35-a).

Table 10. Relative stability with (PMD) + I_o controller with h_1 = 0.1 s.

Gains	Case	G_m	P_m	ω_π	ω_1
k_I =0.6, k_m =0.5	1	2.018	30.8494	17.5549	10.3257
k_I= 0.2883 k_m =0.9439	1	3.9633	56.7727	9.1697	3.1303
k_I=1.0836, k_d=0.05	1	35.2843	92.2099	18.235	0.5897
k_I=0.2883, k_d=0.9439	5	4.2227	56.8796	9.9947	3.2534
k_I=0.2883, k_d=0.9439	9	3.5438	55.3552	9.4709	3.5831

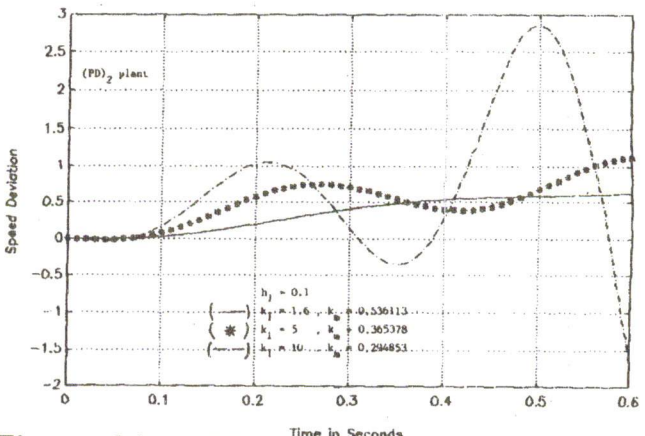

Figure 36-a. C.L. Unstable responses versus optimized one, case 1, (PMD)+I_o Gov.

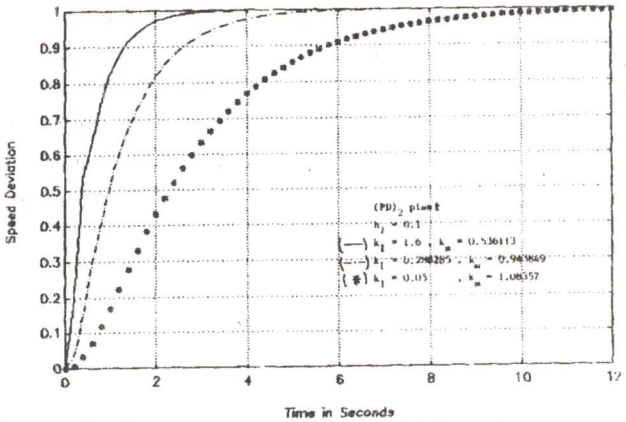

Figure 36-b. Responses -case 1-(PMD)+I_o governor.

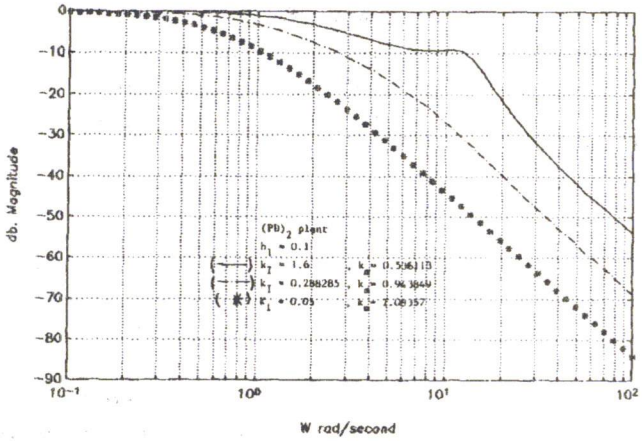

Figure 37-a. CL. Bode plots-various optimized solution, case 1, (PMD)+I_o Gov.

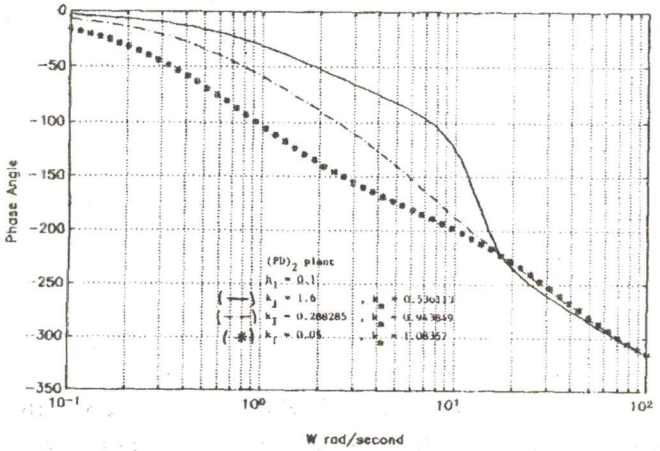

Figure 37-b. CL. Bode plots-various optimized solution, case 1, (PMD)+I_o Gov.

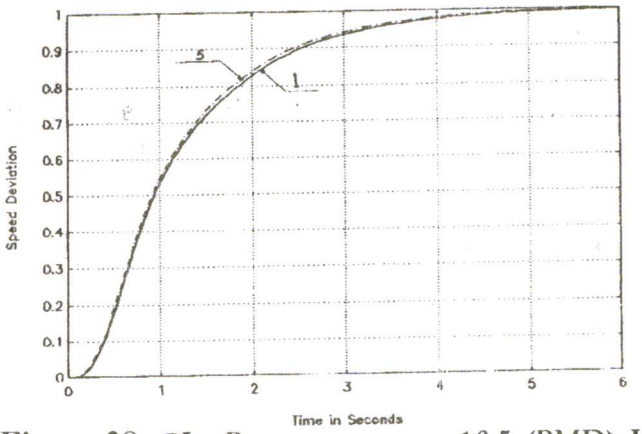

Figure 38. CL. Responses, cases 1&5 (PMD)+I_o Gov., k_I=2883, k_m=0.9439, h_1=0.1.

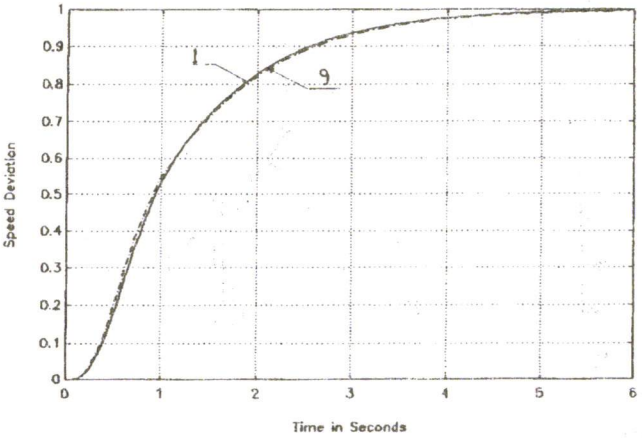

Figure 39. CL. Responses, cases 1&9 (PMD)+I_o Gov., k_I=2883, k_m=0.9439, h_1=0.1.

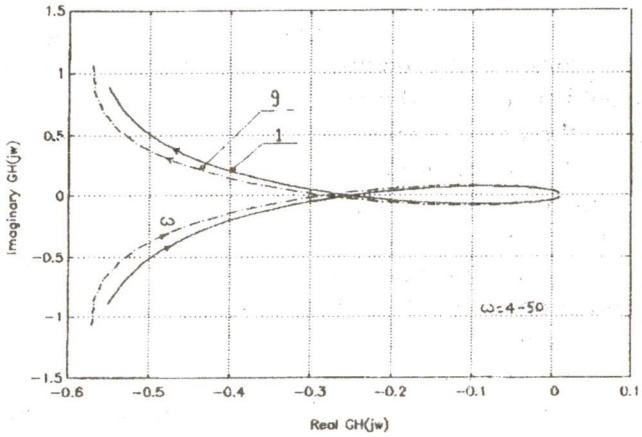

Figure 40. OL. Nyquist plots, cases 1&9 (PMD)+I_o Gov., k_I=2883, k_m=0.9439, h_1=0.1.

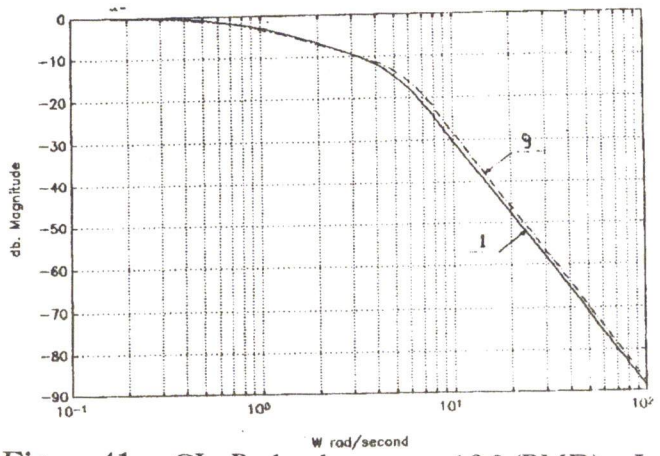

Figure 41-a. CL. Bode plots, cases 1&9 (PMD) + I_o Gov., k_I=0.2883, k_m=0.9439, h_1 = 0.1.

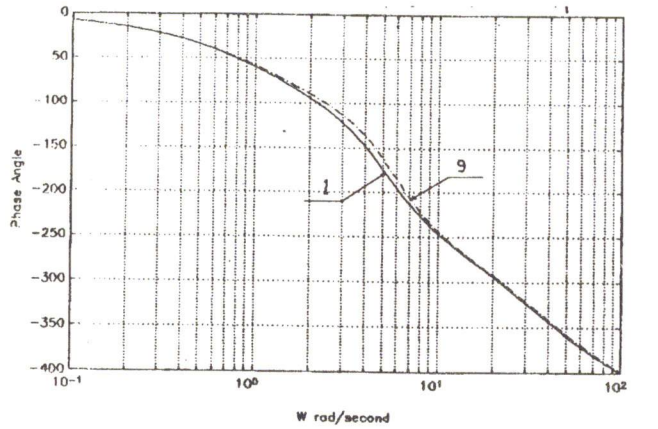

Figure 41-b. CL. Bode plots, cases 1&9 (PMD) + I_o Gov., k_I=0.2883, k_m=0.9439, h_1 = 0.1.

DISCUSSION

When proportional controllers are used for speed governing of the marine Diesel engine, attention should be paid to the value of the proportional gain from the point of view of stability. Inspite that k_p= 4 renders the automatic loop stable with excessive overshoot, the loop becomes unstable if the value of k_p is raised from 4 to 10-Figures (2,3).

when governing the Diesel engine with proportional plus derivative controller (kp= 4, kd = 0.5 s) , decreasing the mean piston speed from (7 to 6 m/s) increases the maximum overshoot and the peak time - Figure (5) , decreases the gain margin and increases the phase margin. On the other hand , both the phase and gain cross- over Frequencies will decrease - Figure (6) and Table (3). A slight deviation is sensed when raising the brake mean effective pressure from (10 to 12 atm.) where the maximum overshoot increases and the peak time decreases.

Oscillatory responses are obtained with increased maximum overshoot and reduced peak time when raising k_p from (4 to 10) and k_d From (0.5 to 1s) . The phenomena of the effect of changing (mps) and (bmp) hold good as mentioned before- Figures (9,11). Regarding the closed loop frequency response, increasing both k_p and k_d increases the resonant peak and resonant frequency. Moreover, increasing the mean piston speed, slightly decreases the resonant peak and increases the resonant frequency - Figures (7,10). Considering Table (3), increasing the value of k_d from (0.5 to 1 s) while holding constant k_p at a value of 4 decreases the gain margin , increases the phase margin while raising both the phase and gain cross -over frequencies.

The optimal linear quadratic regulator designed by the reduced matrix Riccati equation, is characterized by the absence of oscillations, the shorter settling time (about 1s) and the small static error (2%). It should be stated that, the optimal regulator minimizes the time response deviation (with invariant tendency) apart from the reference case- Figures (13, 16) . With Riccati solution, the increase of mean piston speed, increases the gain and phase margins and increases also the phase and gain cross-over frequencies. In contrast to this, the increase of brake mean effective pressure decreases both the gain and phase margins, but increases both ω_π and ω_1 1- Figures (14,17) (and Table (4).If compared with $(PD)_1$ controller , the optimal regulation eliminates too the resonant peak and the corresponding resonant frequency while the bandwidth is kept approximately unchanged- Figures (15,18). Table (5) illustrates the relative stability measures for a typical plant (case 1) with P_1, $(PD)_1$ and optimal regulators where the merits of introducing the derivative gain on the gain and phase margins are obvious. Care should be paid when raising the value of either kp or k_d since the gain margin or both the gain and phase margins may decrease.

Figures from (19 to 24) inclusive , complete the conclusion extracted from Table (5) concerning the

comparisons between the dynamic behaviour of the reference plant with the previous controllers. It can be concluded that an increase in the derivative gain speeds the transient response , increases the maximum overshoot and decreases the peak time while the advantages of the optimal regulator overweigh those of any other controller. In what concerns the closed loop frequency responses, an increase of the derivative gain increases the resonant frequency while there exists a border value of k_d at which the resonant peak is minimum .

The investigation of the dynamic behaviour of the $(PI)_o$ speed governor when operating with the marine Diesel engine are displayed in Figures (26-28) inclusive. In a similar manner, the integral gain k_I is optimized in accordance with the ISE index and Parseval's equation, fixing the proportional gain k_p= 4. Moreover, an arbitrary value of k_I= 5 s^{-1} is chosen too for the objective of comparison . Two solutions are obtained when the ISE criterion is applied that is k_I= 1.6 and 38.8 s^{-1}. The latter value of k_I= 38.8 s^{-1} gives an unstable solution which is attributed to the other constraints imposed on other parameters values of the closed loop. It is evident that the values of k_I= 1.6 s^{-1} can be rather preferred that k_I=5 s^{-1} owing to the facts of less maximum overshoot and less settling time. Nevertheless, the speed of response of the closed loop with k_I= 5 s^{-1} is swifter if compared with the response with k_I= 1.6 s^{-1}.Due to the short time of the transient period without severe fluctuations, the generalized study of the dynamics of cases 1,5 and 9 are be ignored. Considering the relative stability - Table (6), the decrease of k_I from (5 to 1.6 s^{-1}) increases the gain and phase margins, increases ω_π and decreases $\omega_{1\,1}$. Further comments on the closed loop frequency response can be stated that, the increase of the value of k_I increases the value of the resonant peak .

The results of the speed regulation of the marine Diesel engine with Pseudo derivative feedback with optimized values of either k_p or k_d and k_I= 1.6 s^{-1} are indicated in Figures (30-34) inclusive and tables (7,8). The absolute stability investigation is demonstrated in Table (7). It can be shown that an increase of the value of k_p renders the loop unstable, in particular, if accompanied with an increase of the value of k_d. The closed loop transient responses with (PDF) governors, for various values of kp and kd for case 1 are indicated in- Figures (30-a ,b) . In order to meet the requirements of time domain specifications, values of k_p= 0.0136, k_d= 0.5 s and k_I= 1.6 s^{-1} are selected. Apart from the optimal regulator, it can be deduced that with (PDF) control the speed of response is lower than those with (PD) and (PI) controllers . Besides, the (PDF) control is characterized by the non- existence of time domain oscillations , the longest settling time, the smallest bandwidth without resonant peak and, resonant frequency - and the appearance of the influence of transportation lag (infinite order delay) oscillations in closed loop Bode plots .

The orientation of the closed loop transient responses when changing (mps) or (bmp) holds good as in the cases with (PD) and with optimal regulator. The discussion of Table (8) identifies that raising the value of k_p while holding constant the value of k_d reduces the gain and phase margins and decreases too the phase cross-over frequency ω_π. In addition, an augmentation in (mps) enlarges both the gain and phase margins and the corresponding cross-over frequencies ω_π and $_1\omega_1$. Adversely, an increase in the (bmp) decreases both the gain and phase margins and lowers too the corresponding cross-over frequencies ω_π and ω_{11}.

Lastly, the dynamic behaviour of the automatic speed control loop is analyzed with (PMD) control in the feedback path together with an integral control incorporated in the forward path to facilitate the comparison with (PDF) control. A suitable delay time of the controller is selected as h_1 = 0.1 s and optimization according to the ISE index is searched for either by selecting the value of k_I and finding the optimum value of k_m or optimizing both k_I and k_m with the reference plant (case 1) approximated from $(PD)_3$ to $(PD)_2$ by neglecting the fuel delay time $_c$. Table (9) summarizes the obtained values of k_I and k_m while their closed loop transient and frequency responses are displayed in Figures (36 - a,b) and (37 - a,b). As a compromise between the transient response and the relative stability, the established values are as follows: k_m = 0.9439 s, k_I = 0.2883 s^{-1} and h_1 = 0.1 s. With the afore-mentioned settled values, the investigation of the influence of varying (mps) and (bmp) - with the original $(PD)_3$ plant - are portrayed in - Figures (38-41) inclusive. Argumentation of the plots justifies

that in resemblance with the optimal linear quadratic regulator, the (PMD) + I_o control is characterized by the absence of overshoots, prompt speed of response, short setting time, small bandwidth, the non-existence of resonant peak or resonant frequency and the rectification of oscillations caused by the dead time in closed loop Bode plots. It can be safely concluded that the optimized (PMD) + I_o control minimizes the deviations apparent with conventional controllers due to changes in engines parameters such as (mps) and (bmp). Just next to the optimal regulator, parameter-optimized control with (PMD) + I_o may be regarded as the best regulation surpassing the merits of (PDF) control which in turn, excels the merits of (PD) and (PI) conventional controllers. Scanning the results shown in Table (10) assures the results got before namely, the increase of (mps) increases both the gain and phase margins whereas the increase of (bmp) decreases both the gain and phase margins. Table (10) certifies too, that w.r.t. the degree of stability, apart from the optimal regulator - which insures the highest gain and phase margins, the optimized (PMD) + I_o control possesses considerably spacious gain and phase margins which outweigh those obtained with optimized (PDF), (PI) and (PD) controllers.

CONCLUSION

Dynamic behaviour of speed regulating systems of marine Diesel engines is analyzed. The analysis involves absolute and relative stability, transient and frequency responses. Controllers in concern for investigation are proportional, proportional-derivative,parameter-optimized proportional-integral, pseudo derivative feedback and proportional minus delay plus integral control and optimal linear quadratic regulators. Merits of optimal and parameter-optimized non-conventional controllers over the traditional types are evident. The former regulators capture the distinguishing properties of the latter types and exclude their unwanted drawbacks.

The effect of diverse controllers parameter variations beside changes in engine's mean piston speed and brake mean effective pressure is discussed.

Setting aside the optimal regulator which represents the most adequate one, the proportional minus delay plus integral control, then the pseudo derivative feedback control can be judged to be confidently advantageous and possess agreeable performances. Besides, narrow deviations in responses are noticed if the prementioned non-traditional controllers are adopted when the engine undergoes parameters variation. Owing to the dead and delay times inherent in the plant, it is not easy to regulate it with a proportional controller. An uncomputed increase in its gain or unforeseen severe nature disturbance may render the automatic loop unstable. Should other conventional controllers be used, the question of selecting either proportional-derivative or proportional-integral regulator and how much should be their gains, depends on meeting the significant control requirements in what concerns the speed of response, the maximum overshoot, the peak and settling times, the bandwidth , the resonant peak and frequency together with taking into account the plant dynamics and the nature of perturbation.

It can be concluded that, as a general tendency, the increase of the controller derivative gain improves the speed of response, reduces the settling time but raises the maximum overshoot and decreases the peak time. In contradiction to time domain performance, the increase of the derivative gain reduces the measures of the degree of stability.

With parameter-optimized (PI) control, the reduction of the integral gain lowers both the speed of response and the maximum overshoot, speeds the settling time, improves the relative stability and decreases the resonant peak. If parameter-optimized (PDF) control is chosen, the time domain oscillations disappear, associated with a slowish speed of response, long settling time, small bandwidth and the non-existence of resonant peak and frequency.

Furthermore, control with (PMD) + I_o yields prompt speed of response, absence of overshoots, short settling time, small bandwidth and the elimination of both resonant peak and frequency. Lastly, a generalized orientation is recorded that the increase of mean piston speed improves the relative stability indicators while on the contrary, the increase of brake mean effective pressure injures these measures.

REFERENCES

[1] S. Youssef, M. Hanafi and M., Morsy," *Speed Control of Marine Diesel Engines -A parametric analysis"*, Presented to AEJ.

[2] R. Szaday, ."*Szabayozaselmélt Elemei"*, Müszaki Konyv Kiado, Budapest, 1972 .

[3] A. Ulsoy, "*Optimal Pseudo- Derivative feed back control"*, M.S. Thesis, Cornell Univ., Ithaca, New York, 1975 .

[4] J.N. Plam III, " *Cont Systems Engineering* ", John Wiley & Sons , New York , 1986.

[5] H. Suh and Z. Bien, " *Use of Time Delay Actions in Controller Design* ", IEEE Trans. on Aut. Cont. vol. , AC-25, No.3, June 1980.

[6] E. Jury, *A Note on The Evaluation of The Total Square Integral.*", IEEE Trans. On Aut. Cont., vol. AC-10, No.1, Jan. 1965, pp.110-111.

[7] E. Jury and A. Dewey, " *A General Formulation of The total Square Integral For Continuous Systems*", IEEE Trans. On Aut. Cont., vol. AC-10 No.1 Jan., 1965, PP 119-120.

[8] I. Nagarath M. Gopal, " *Control Systems Engineering*", John Wiley & Sons, New York, 1982.

[9] M. Hanafi and A.M. El-Iraki, "*Optimized Parameter Versus Optimal Controllers for Marine Diesel Engines*", AEJ. July, 1994.

[10] El- Iraki, A.M. and Hanafi, M. " *Investigation on Non - Conventional PMD Control'* , AEJ. July, 1994.

[11] _____ , Mathematica, Ver. 2.1 For Windows- A System for Doing Mathematics by Computer, Wolfram Research, Inc. U.S.A., 1993.

[12] _____ ," *MATLAB 4.0, for Windows*," The Mathworks Inc., stanford U.S.A., 1993.